UV-femtosecond laser ablation of SrTiO3 single crystals

IOP Publishing Journal of Physics: Conference Series **59** (2007) 610–615
doi:10.1088/1742-6596/59/1/130 Eighth International Conference on Laser Ablation

UV-femtosecond laser ablation of $SrTiO_3$ single crystals

S Zoppel[1,3], D Gray[2], M Farsari[2], R Merz[3], G A Reider[1] and C Fotakis[2]

[1]Vienna University of Technology, Photonics Institute, Gusshausstr. 27-29/387, 1040 Vienna, Austria
[2]Foundation for Research and Technology – Hellas, Institute of Electronic Structure and Laser, P.O. Box 1527, 71110 Heraklion, Crete, Greece
[3]Vorarlberg University of Applied Sciences, Research Center for Microtechnologies, Achstrasse 1, 6850 Dornbirn, Austria

Abstract. We have investigated the ablation behaviour of single crystal $SrTiO_3$ <100> with focus on the influence of the pulse duration at a wavelength of 248 nm. The experiments were performed with KrF-excimer lasers with pulse durations of 34 ns and 500 fs, respectively. Femtosecond-ablation turns out to be more efficient by one order of magnitude and to eliminate the known problem of cracking of $SrTiO_3$ during laser machining with longer pulses [1],[2]. In addition, the cavities ablated with femtosecond pulses display a smoother surface with no indication of melting and well-defined, sharp edges. These effects can be explained by the reduced thermal shock effect on the material by using ultrashort pulses.

1. Introduction

Because of their electrical properties, from insulating to semi conducting and even metallic-like behaviour, perovskites like $SrTiO_3$ are of great practical interest for modern electronic devices or as substrates in thin film technology. $SrTiO_3$ is paraelectric and maintains the perovskite crystal structure over a wide temperature range. Its large dielectric constant and high dielectric breakdown field makes $SrTiO_3$ a potential candidate for storage capacitor cells in next-generation dynamic random access memories [3]. Because of these outstanding features, micro patterning of $SrTiO_3$ and laser machining in particular is of great interest. Earlier studies carried out with nanosecond lasers [1],[2], however, have shown that laser machining of $SrTiO_3$ suffers from the formation of surface cracks (Figure 1).

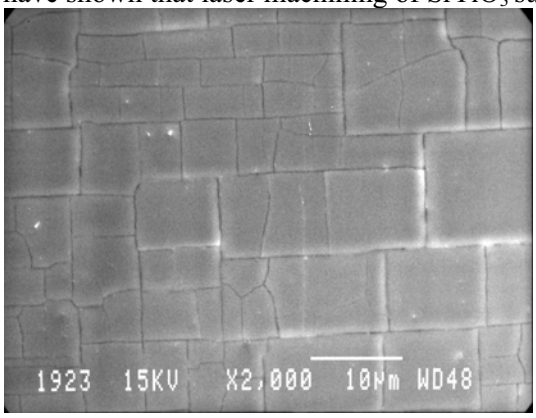

Figure 1. Cracks along the crystallographic axis after 50 pulses with a fluence of 4,89 J/cm^2, λ = 248 nm, τ = 34ns

The parameters which significantly influence the ablation interaction process are the wavelength and the pulse duration of the ablation laser. Because of the wide bandgap of $SrTiO_3$ short wavelength radiation is required to allow ablation based upon linear absorption.

Most work on single-crystal oxides (MgO [4]-[6], $SrTiO_3$ [1],[2],[7]) found in literature has therefore been carried out with lasers emitting in the UV, with pulse durations in the nanosecond timescale. Ablation studies with ultrafast (femtosecond) UV lasers have been carried out on various materials, predominantly on polymers [8]-[11], but also on dielectric materials [12],[13] and semiconductors [14]. The potential of those systems for microstructuring, even in the submicron range, has been shown by Chen, Klein and others [15]-[17]. As with ultrafast IR-lasers [18], the physically different mechanism of ultrafast (non-thermal) ablation has been shown to improve the ablation process considerably.

In this paper we show the ablation behavior of $SrTiO_3$ by employing ultrashort pulses in the UV. The differences in morphology and in the ablation parameters depending on the pulse duration are presented.

2. Experimental

The two lasers employed are a KrF-Excimer laser (LPX 200, Lambda Physik) with a pulse duration of 34 ns and a wavelength of 248 nm, and a distributed feedback dye laser system pumped and amplified by this same laser, yielding 500 fs pulses at 248 nm, respectively. In the nanosecond excimer laser experiments, a (circular) iris aperture was placed in the beam path and imaged by means of a single lens with a focal length of 60 mm. The sample, which was fixed on a xyz-stage, was positioned in the image plane of this lens system. For the femtosecond experiments, the sample was positioned several millimeters before the focus plane to avoid electrical breakdown in air. The beam diameter at the sample position was 250 microns. In both cases the intensity of the beam was adjusted with a reflecting variable attenuator and all experiments were done under ambient conditions.

The samples used were single crystal $SrTiO_3$ <100>, polished on one side. It has a bandgap of 3.2 eV, corresponding to a wavelength of 388 nm. The ablated cavities were measured with a Tencor Alphastep 100 to determine the ablation rate. The surface morphology of the ablated cavity and its surroundings were observed by a scanning electron microscope. XRD (X-Ray Diffraction) measurements have been carried out to obtain information about possible structural changes by the mechanical load during exposure with fluences below the multi-pulse ablation threshold.

3. Results and Discussions

Because of the radial variation of the ablation depth which results from the inhomogeneous energy distribution of the femtosecond laser beam, the volume of the ablated cavity was calculated on the base of a radial cross section of the ablated area provided by the Alphastep profilometer, assuming a rotational symmetry of the cavity. To allow for a direct comparison with other experiments, an effective ablation rate (nm/pulse) was extracted from these values. Each cavity was ablated with a train of 100 pulses at a repetition rate of 4 Hz.

A comparison between the nanosecond and femtosecond ablation rate is shown (Figure 2). In the case of ablation with nanosecond pulses the ablation rate increases linearly with the pulse energy. For the femtosecond experiments, there is evidence of a saturation effect at higher fluences which is well known for ultrashort ablation [19]. Due to the high peak intensities critical plasma effects may occur, that prevent further energy deposition into the target. To obtain conclusive information about these effects, however, ablation studies at higher fluences would be necessary. While the above-bandgap photon energy permits ablation by a single photon process, there is still a large benefit from using sub-picosecond pulses because of the reduced thermal diffusion during the exposure time.

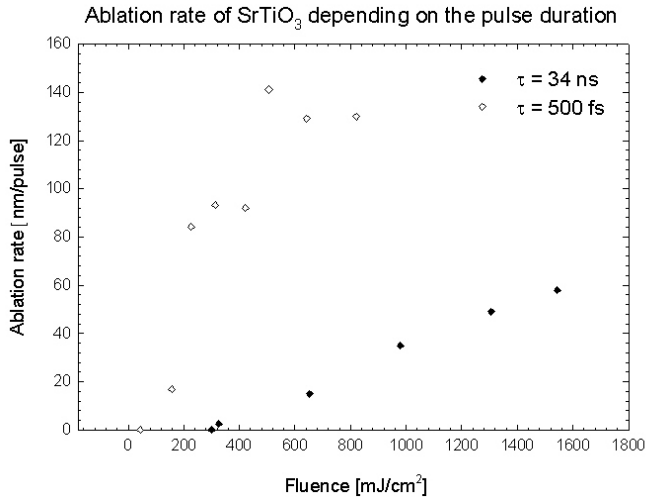

Figure 2. Comparison of the ablation rate for a wavelength of 248 nm at pulse durations of 34 ns and 500 fs, respectively.

For both laser systems the ablation thresholds for single-pulse and multi-pulse treatment was determined (Table 1). The ratio between the single- and multi-pulse ablation threshold is about 3.5 in the case of femtosecond ablation and significantly smaller (about 2) for the nanosecond experiments. The decreased ablation threshold for multi-pulse treatment can be attributed to an accumulation of defects caused either by multiphoton creation of microscopic defects (femtosecond regime,[20],[21]) or to stress induced defects created by the repetitive heating/cooling cycles (nanosecond regime). In all likelihood, the different mechanism and the possibility of partial annealing of defects in the nanosecond regime are responsible for the different multi- to single-pulse threshold ratios.

Table 1. Determined single-pulse and multi-pulse ablation thresholds for the used pulse durations at a wavelength of 248 nm

Pulse duration	Ablation threshold (J/cm²)	
	Single pulse	Multi pulse (N=100)
35 ns	0,6	0,3
500 fs	0,15	0,044

For multi-pulse ablation with femtosecond pulses the value is approximately one order of magnitude lower compared to the nanosecond results. The much lower threshold fluence and enhanced ablation yield are both due the fact that for sub-picosecond UV pulses the laser energy is deposited within the optical penetration depth of approx. 13 nm (n = 2.085 + j1.474 at 245 nm wavelength [22]) while it spreads, via thermal diffusion, into a much deeper volume during nanosecond irradiation (thermal diffusivity of 35.8×10^{-7} m^2/s yields a thermal diffusion length of 350 nm at our pulse duration [23]). The ablation rate of the femtosecond pulses is smaller or comparable to the optical penetration depth for low fluences. With increasing intensity the optical properties of the illuminated material change in an unknown fashion due to nonlinear optical effects so that a simple comparison to the penetration depth is no longer possible.

In the case of ns ablation and depending on the laser intensity various detrimental effects could be observed that are due to the thermal nature of the ablation process. At a fluence of 0.2 J/cm^2 darkening of the irradiated area occurs after a single pulse, which may be due to a chemical modification of the surface region. More strikingly, higher fluences lead to the formation of cracks along the crystallographic axis. This effect has also been mentioned in an earlier study with ns pulses [1]. In Figure 3 a section of an ablated area is shown after 50 pulses at a fluence of 4.89 J/cm^2.

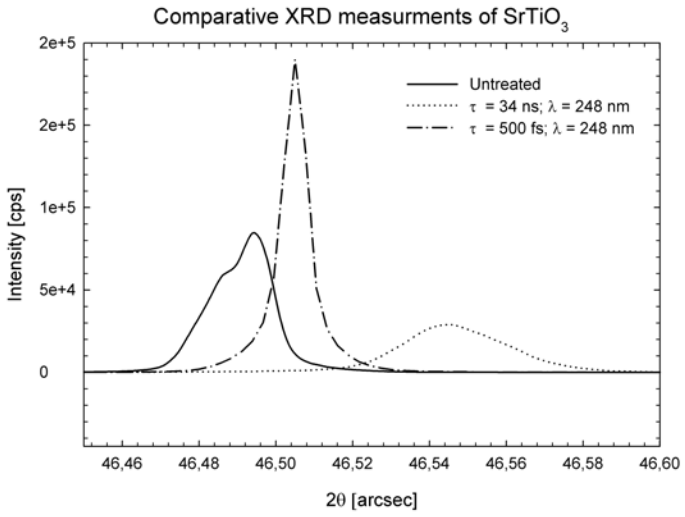

Figure 3. XRD-measurement of $SrTiO_3$. The samples have been exposed with fluences just below the ablation threshold.

The cracks look shingle type and their size is varying from approximately three up to twenty microns. The threshold fluence for the crack formation is 0.3 J/cm^2, which is below the ablation threshold of 0.6 J/cm^2 for single pulse irradiation. The cracks appeared over the whole energy range used for the single pulse experiments (0.3-7 J/cm^2).

After a hundred pulses the effect of cracking could still be observed but it starts to disappear at fluences higher than 0.7 J/cm^2, which we attribute to partial thermal annealing. Despite the annealing, a significant residual distortion of the crystal lattice remains, as outlined below. In the case of ultra short pulses neither darkening nor formation of cracks could be observed at any fluence neither for single- nor for multi-shot irradiation.

The formation of the cracks has been attributed to a thermal process comprising shockwave excitation in the material [18]. Although the photon energy (5eV) used is high, thermal interactions seem to predominate on the nanosecond timescale. As $SrTiO_3$ is a bad heat conductor (12 Wm^{-1}K^{-1}) and the melting/boiling points are very high (2080°C and >3000°C, respectively), an excessive temperature gradient, resulting in thermal shock, is induced in the surrounding material which leads to the cracking of the material along the crystallographic planes.

On the femtosecond time scale the ablation process is faster than the energy transfer into the bulk material. So nearly all of the energy deposited by the laser pulse is used for the material removal and carried away by the ablation products. Because of the negligible heat transfer into the material bulk, the thermal shock is avoided.

X-Ray diffraction (XRD) measurements have been carried out after exposure of the samples with fluences below the multi pulse ablation threshold. In the graph of the untreated surface is juxtaposed with results from areas irradiated with femto- and nanosecond pulses, respectively.

Sample areas exposed to nanosecond pulses display a shift of the diffraction peak to the right indicating compressive strength. The shift resulting after femtosecond irradiation is much smaller indicating the much lower mechanical load on the material.

Besides the effect of cracking, additional differences in morphology can be seen by comparing the ablated cavities. Figure 4 shows scanning electron micrographs of areas ablated with hundred shots at fluences of 3.3 J/cm^2 and 1.3 J/cm² at pulse durations of 34 nanoseconds and 500 femtoseconds, respectively. Both ablated structures provide comparable values of ablation rate. For the nanosecond pulses the corrugated shape of the bottom area most likely results from the annealing of the afore mentioned cracks by melting and resolidification of the material. The bottom also shows pores with a size of approximately 300 to 800 nm, which is also an evidence of a melting process. Their appearance is significantly more abundant at the partially annealed, but still distinguishable cracks. The sidewalls are smooth and in addition, the lower edge is very sharp. In comparison to ablation with femtosecond

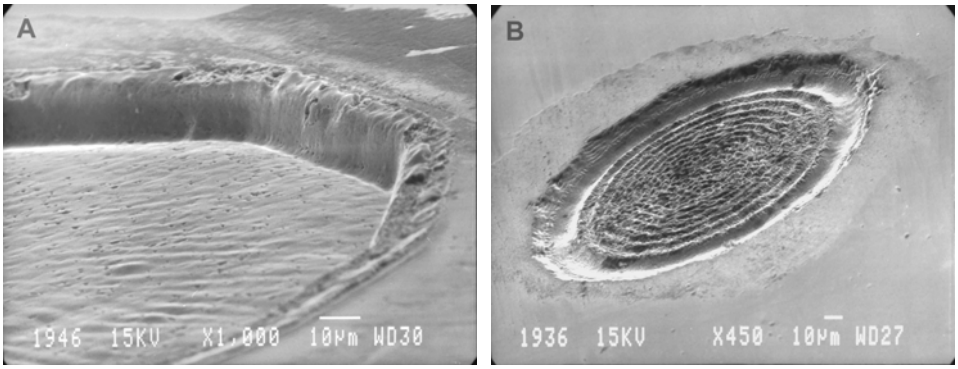

Figure 4. Cavities in $SrTiO_3$ ablated with a wavelength of 248 nm and pulse durations of 34ns (A) and 500 fs (B), respectively. The spots have been exposed with 100 pulses at a fluence of 3.3 J/cm² for the nanosecond and 1,3 J/cm² for the femtosecond experiments.

pulses, showing in image B, the surrounding area is more affected due to the higher heat transfer into the bulk material. The upper edge is rounded and the transition to the unexposed area shows ejected material and a rough surface indicating thermal damage. In contrast to this, the SEM micrograph of the femtosecond ablated structure shows no indication of melting. It exhibits sharp edges and less debris deposited at the surrounding area. The pores mentioned before could not be observed when using femtosecond pulses. The corrugated surface is a replica of the intensity distribution of the laser beam (which is a diffraction pattern of the circular aperture used for beam shaping).

4. Conclusion

The known problem of cracking of $SrTiO_3$ during laser machining with nanosecond UV pulses can be avoided by using pulses in the femtosecond time scale. The formation of cracks is the result of a thermal shock affecting the material when using nanosecond pulse durations. In addition, femtosecond ablation turns out to be more efficient by one order of magnitude in comparison to laser ablation with longer pulse durations. The cavities ablated with femtosecond pulses show no indication of melting and exhibit smooth and well-defined surfaces and edges.

Acknowledgements

Sandra Zoppel has been supported by a fellowship (HPMT-GH-00-00177-20) from the Marie Curie Training Site operating at IESL-FORTH, under the European Commission Human Potential program. Parts of the work have been supported by the FHplus impulse program from the BMVIT.

References

[1] Benitez F, Sanchez F, Trtik V, Varela M, Bibes M, Martinez B and Fontcuberta J 1999 *Appl.Phys.A* **69**, 501-4
[2] Most D, Choi J, Belenky L J and Eom C B 2003 *Solid-State Electronics* **47**: 2249-53
[3] Shibuya K, Ohnishi T, Lippmaa M, Kawasaki M and Koinuma H 2004 *Appl. Phys. Lett.* **85**(3), 425-427
[4] Dirnberger L, Dyer P E and Farrar S R 1993 *Appl. Surf. Science* **69**(1-4): 216-20
[5] Dickinson J T, Jensen L C and Webb R L 1993 *J. Appl. Phys.* **74**(6): 3758-67
[6] Webb R L, Jensen L C and Langford S C 1993 *J. Appl. Phys.* **74**(4): 2323-37
[7] Ishibashi H, Arisaka S, Kinoshita K and Kobayashi T 1994 Jpn. *J. Appl. Phys.* **33**(9A): 4971-7
[8] Adhi K P, Owings R L, Railkar T A, Brown W D and Malshe A P 2004 *Appl. Surf. Science* **225**, 324-31
[9] Beinhorn F, Ihlemann J, Luther K and Troe J 2004 *Appl. Phys. A* **79**, 869-73
[10] Athanassiou A, Lassithiotaki M, Anglos D, Georgiou S and Fotakis C 2000 *Appl.Surf. Science* **154-155**, 89-94

[11] Bityurin N and Malyshev A 2002 *J. Appl. Phys.* **92**(1), 605-13
[12] Ihlemann J and Wolff-Rottke B 1996 *Appl. Surf. Science* **106**, 282-6
[13] Ihlemann J, Scholl A and Schmidt H 1995 *Appl. Phys. A* **60**(4), 411-7
[14] Simon P and Ihlemann J 1996 *Appl Phys. A* **63**,505-8
[15] Chen K and Ihlemann J 1997 *Appl.Phys. A* **65**, 517-8
[16] Klein-Wiele J H, Bekesi J and Simon P 2004 *Appl. Phys. A* **79**, 775-8
[17] Chen K, Ihlemann J, Simon P, Baumann I and Sohler W 1997 *Appl. Phys. A* **65**, 517-8
[18] Perry M D, Stuart B C, Banks P S, Feit M D, Yanovsky V and Rubenchik A M 1999 *J. Appl. Phys.* **85**(9), 6803-10
[19] Guizard S, Semerok A, Gaudin J, Hashida M, Martin P and Quéré F 2002 *Appl. Surf. Science* **186** 364-8
[20] Ashkenasi D, Lorenz M, Stoian R and Rosenfeld A 1999 *Appl. Surf. Science* **150** (1-4), 101-6
[21] Bonse J, Baudach S, Krüger J, Kautek W and Lenzner M 2002 *Appl. Phys. A* **74**, 19-25
[22] Martinez E, Garcia S, Marin E, Vassallo O, Pena-Rodriguez G, Calderon A and Siqueiros J M 2004 *J. Mat. Science* **39**, 1233-39
[23] Bäuerle S, Braun E, Saile V, Sprussel S and Kock E E 1978 *Z. Phys. B* **18**, 5177